PHYSICAL REVIEW B **79**, 060506(R) (2009)

Microstructure and tetragonal-to-orthorhombic phase transition of AFe_2As_2 (A=Sr,Ca) as seen via transmission electron microscopy

C. Ma, H. X. Yang, H. F. Tian, H. L Shi, J. B. Lu, Z. W. Wang, L. J. Zeng, G. F. Chen, N. L. Wang, and J. Q. Li*
Beijing National Laboratory for Condensed Matter Physics, Institute of Physics, Chinese Academy of Sciences, Beijing 100080, China
(Received 6 January 2009; revised manuscript received 12 January 2009; published 11 February 2009)

The structural properties of the AFe_2As_2 (A=Sr,Ca) compounds have been extensively analyzed by transmission electron microscopy (TEM) from room temperature down to 20 K. The experimental results demonstrate that the $SrFe_2As_2$ compound, consistent with the previous x-ray data, undergoes a visible tetragonal-to-orthorhombic (T-O) phase transition at low temperature. Moreover, twinning lamellae arising from T-O transition clearly appear in the orthorhombic phase. On the other hand, TEM observations of $CaFe_2As_2$ reveal the presence of a pseudoperiodic structural modulation with a periodicity of around 40 nm at room temperature. This modulation is likely related to the local structural distortions within the Ca layers. *In situ* cooling TEM observations of $CaFe_2As_2$ reveal the presence of complex domain structures in the low-temperature orthorhombic phase.

DOI: 10.1103/PhysRevB.79.060506 PACS number(s): 74.70.Dd, 61.05.J−, 61.50.Ks

Following the discovery of superconductivity at $T_c \approx 26$ K in LaFeAsO(F),[1] a variety of ZrCuSiAs-type (1111 phase) superconductors with T_c ranging from 2 to 55 K have been discovered, such as $RFeAsO_{1-x}F_x$,[2–4] $RFeAsO_{1-\delta}$,[5] and $R_{1-x}A_xFeAsO$ (Ref. 6) (R=La,Ce,Pr,Nd,Sm,Gd,Tb; A=Sr,Ca). Similar to the high-temperature cuprate superconductors, the (Fe_2As_2) layers are considered to be the conducting layers and play a critical role in the understanding of superconductivity in this kind of materials, while the (R_2O_2) layers inject charge carriers to the former via chemical doping. Furthermore, the AFe_2As_2 (A=Ca, Sr, Ba, and Eu) compounds of the $ThCr_2Si_2$-type structure (122 phase) are found to be also superconductors under certain conditions, e.g., partial substitution of K (or Na) for A atoms and application of hydrostatic pressure.[7–11] The highest superconducting T_c in this family is found to be about 38 K in $Ba(K)Fe_2As_2$.

Recent structural and physical investigations have documented that the (FeAs)-based system contains noteworthy competition among numerous ordered states depending remarkably on doping charge carriers. The ROFeAs and AFe_2As_2 parent compounds in general show, respectively, remarkable anomalies in physical properties between 120 and 220 K as commonly observed in measurements of their electrical resistivity and magnetic susceptibility. These anomalies are found to be associated with the spin-density wave (SDW) instability and tetragonal-to-orthorhombic (T-O) phase transition at low temperature.[12–15] Measurements of structural and physical properties of $BaFe_2As_2$, $SrFe_2As_2$, and $CaFe_2As_2$ suggest that the phase transitions occur at about 140, 205, and 170 K, respectively, as shown in Fig. 1. Neutron and x-ray diffraction studies demonstrate that this phase transition can be well characterized as tetragonal $I4/mmm$ to orthorhombic $Fmmm$ structure.[16–22] In order to directly reveal the structural changes associated with this phase transition, we carried out a series of *in situ* transmission electron microscopy (TEM) observations on AFe_2As_2 samples from room temperature down to 20 K. In this paper, we report our TEM results obtained in recent investigations; both the pseudoperiodic modulation in $CaFe_2As_2$ and structural twinning arising from T-O phase transition in $SrFe_2As_2$ are systematically analyzed.

The AFe_2As_2 single crystals used in the present study were prepared by the high-temperature solution method[12,23] using FeAs as flux. The starting materials of Sr (Ba or Ca) and FeAs in a ratio of 1:4 were put into an alumina crucible and then sealed in an evacuated quartz ampoule and heated at 1175 °C for 5 h and then cooled slowly to 1000 °C for over 50 h. We finally got the platelike single crystals with the size ranging from 3 to 6 mm. Specimens for TEM observations were prepared by peeling off a very thin sheet, a few tens of microns thick, from the single crystal and then followed by ion milling. In addition, we also prepared some samples for electron-diffraction experiments simply by peeling off fine fragments from the layered single crystals which were dissolved in chloroform and then supported by a copper grid coated with a thin carbon film. Microstructure analyses were performed on a FEI Tecnai-F20 TEM equipped with double-tilt cooling holders.

We first focus on the microstructure and changes of structural properties associated with the low-temperature T-O phase transition in $SrFe_2As_2$ and $BaFe_2As_2$. Despite the different T-O transition temperatures of these two compounds, our TEM observations reveal that these two samples show very similar microstructural changes with lowering temperature, therefore, we mainly focus on the experimental results

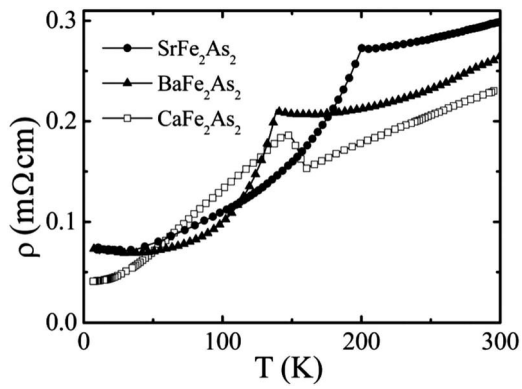

FIG. 1. Electric resistivity vs temperature of AFe_2As_2 (A=Sr, Ba, and Ca).

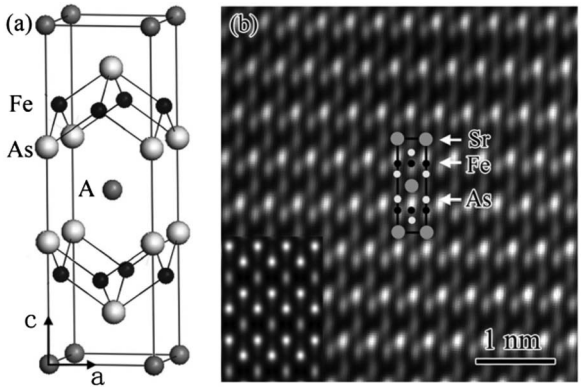

FIG. 2. (a) Crystal structure of AFe_2As_2 (A=Sr, Ba, and Ca). (b) High-resolution TEM image for $SrFe_2As_2$ sample taken along the [100] zone-axis direction at room temperature. The structural model is superimposed on the image, and the black rectangle represents a unit cell. Inset shows a simulated TEM image.

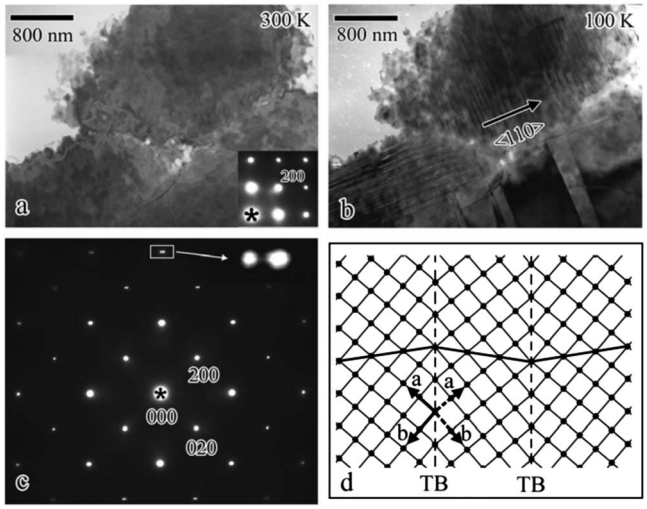

FIG. 3. Bight-field images for $SrFe_2As_2$ sample taken at (a) 300 K and (b) 100 K, respectively. Inset in (a) shows the corresponding electron-diffraction pattern. (c) Electron-diffraction patterns taken along the [001] zone-axis direction at 100 K. Inset shows enlarged (400) Bragg spot with spot splitting along the $\langle 110\rangle_{orth}$ direction. (d) Schematic structural model illustrating twins within an Fe layer. TB represents twin boundary.

obtained from $SrFe_2As_2$ in the following discussions. $SrFe_2As_2$ has a tetragonal structure at room temperature, as schematically shown in Fig. 2(a). Figure 2(b) displays a high-resolution TEM image taken along the [100] zone-axis direction, illustrating the layered structural feature of AFe_2As_2. This image was obtained from a thin area nearly under the Scherzer defocus; the dark dots, therefore, represent the atomic positions as clearly indicated in the structural model superimposed on the experimental image. High-resolution TEM image simulations for $SrFe_2As_2$ were carried out by varying the sample thickness from 2 to 5 nm and the defocus value from −30 to −60 nm. A simulated image with a defocus value of −45 nm and a thickness of 3 nm is superimposed on the experimental image and appears to be in good agreement with the experimental one. On the other hand, it is noted that the distance between Fe and As columns (~0.14 nm) in the present case is noticeably smaller than the spatial resolution of our TEM (0.2 nm). Hence, the positions of Fe and As atoms cannot be clearly distinguished in this experimental image. A further structural study using a Cs-corrected TEM is in progress for directly characterizing the atomic structural feature within the FeAs layers.

The $SrFe_2As_2$ compound in general shows a structural phase transition at about 205 K, associated with spin-density wave instability.[12,15] In order to directly observe the structural changes following this phase transition, we performed a series of *in situ* TEM investigations on well-characterized single crystalline $SrFe_2As_2$ samples. Figures 3(a)–3(c) show the bright-field TEM images and corresponding electron-diffraction patterns taken along the [001] zone-axis direction at 300 and 100 K, respectively, illustrating the typical structural changes in $SrFe_2As_2$ through the T-O phase transition. Similar structural changes were also observed in $CaFe_2As_2$ as discussed in the following context. Moreover, microstructure observations demonstrate that the low-temperature orthorhombic $SrFe_2As_2$ is heavily twinned, with the $(110)_{orth}$ plane being its twinning plane. The a and b orthorhombic axes are mirrored across the twin boundary [Fig. 3(d)]. We herein used different space groups for describing the tetragonal and orthorhombic structures, i.e., the a and b axis directions in the orthorhombic phase are parallel to the [110] and [−110] directions in the tetragonal phase, respectively. Figure 3(b) shows a typical bright-field TEM image illustrating the twinning lamellae in a $SrFe_2As_2$ sample. The width of twinning domains, often depending visibly on temperature, ranges from 100 to 400 nm at 100 K. Actually there are many factors that could affect the twin density, such as thermal treatments, impurity content, and sample preparation techniques. The exact atomic structure of the twin boundaries in $SrFe_2As_2$ has not yet been determined. Considering the simultaneous occurrence of the SDW instability and T-O phase transition, we propose a schematic structural model illustrating twins within an Fe layer, as shown in Fig. 3(d). The [001] zone-axis electron-diffraction pattern obtained from several twin domains clearly shows the difference in the lattice parameters (a and b) as spot splitting along the $\langle 110\rangle_{orth}$ direction, as shown in Fig. 3(c). The orthorhombic splitting angle in the present case, estimated from the electron-diffraction pattern, is given by $\alpha=2[tg^{-1}(a/b) - 45°] \approx 1°$, where a and b are lattice parameters for the orthorhombic phase. Therefore, the ratio of the lattice parameter a/b is expected to be about 1.009, which is fundamentally in agreement with the data of the x-ray and neutron diffractions ($\approx$1.010).[15]

We now proceed to study the microstructure and structural phase transition in $CaFe_2As_2$. Figure 4(a) shows a bright-field TEM image taken from a $CaFe_2As_2$ sample with tetragonal structure at room temperature. The striking structural feature, in contrast with that of $BaFe_2As_2$ and $SrFe_2As_2$, is the appearance of a pseudoperiodic modulation along the tetragonal [110] direction; the average wavelength of this modulation is estimated to be about 40 nm. The periodicity of this modulation usually does not vary notably from one area to another. Regular contrast of modulation stripes can be

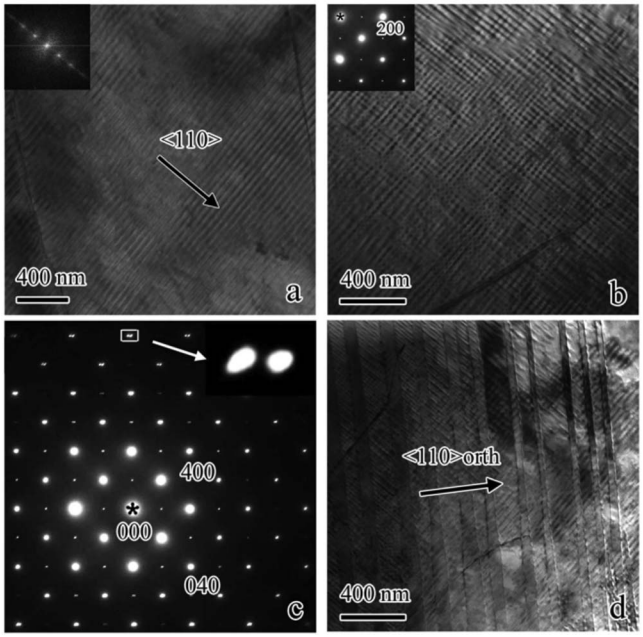

FIG. 4. Bright-field images of $CaFe_2As_2$ taken at room temperature, showing a (a) pseudoperiodic modulation and (b) a tweed structure. Insets in (a) and (b) show, respectively, the FFT for the TEM images and corresponding electron-diffraction pattern. (c) Electron-diffraction patterns of $CaFe_2As_2$ taken along the [001] zone-axis direction at 100 K. Inset shows enlarged (600) Bragg spot with clear spot splitting along the $\langle 110\rangle_{orth}$ direction. (d) Bright-field image of $CaFe_2As_2$ taken at 100 K, showing a mixture of the tweed and twin domains.

often observed in many crystals. Moreover, this kind of modulation stripes can commonly coexist along two equivalent [110] and [−110] directions, and two orthogonal modulations overlap (meet) to yield an interesting pattern as shown in Fig. 4(b). This type of microstructure feature of lenticular domains can be called as a "tweed" structure as commonly observed in many alloys[24] and in the Fe-doped $YBa_2Cu_3O_{7-x}$ superconductor,[25] in which the tweed structure arises from the compositional disorder or local lattice distortions. The inset in Fig. 4(a) is the data of the fast Fourier transformation (FFT) for the TEM image, showing clear superstructure reflections following the direct spot corresponding to the structural modulation. In order to confirm that this pseudoperiodic modulation is essentially a bulk effect rather than a stress-driven feature during sample thinning, we therefore have prepared TEM samples using different methods and the results demonstrated that all samples clearly show the similar tweed structure in both thick and thin areas.

It is remarkable that the Bragg spot at the systematic (100) position, which should be absent according to the space group $I4/mmm$, is often obviously observable in the electron-diffraction pattern, as shown in the inset in Fig. 4(b). The presence of the (100) reflection spot cannot be attributed to multiple diffraction effects, but arises from a notable alteration of local crystal symmetry related to both the structural modulation and the tweed structural domains. Because no evident spots splitting or streaking in the electron diffraction are observed at room temperature, the local orthorhombic distortion in $CaFe_2As_2$ must be rather small within the a-b plane.

Like the $SrFe_2As_2$ sample, the $CaFe_2As_2$ sample, following with the T-O phase transition at about 170 K, also adopts an orthorhombic structure at low temperature. Our *in situ* cooling TEM study demonstrates that this T-O transition is well characterized by the unambiguous spot splitting [Fig. 4(c)] and the formation of twin boundaries [Fig. 4(d)]. The sharp contrasts of parallel lines along the $[110]_{orth}$ direction are twin boundaries. Actually, the low-temperature TEM image often exhibits complex microstructures with coexistence of a twin domain structure and a tweed structure. The twin boundary makes an angle of around 45° with the pseudoperiodic modulation. The twin boundary in the orthorhombic phase goes along the diagonal of the iron squares, i.e., the $[110]_{orth}$ or $[-110]_{orth}$ direction as similarly discussed for $SrFe_2As_2$ in the above context. The width of the domain (100–500 nm) is much larger than that of the modulation stripes (~40 nm) that exist at room temperature. It is also noted that the observed microstructure features in $CaFe_2As_2$ along with the T-O transition are much different from those observed in $YBa_2Cu_3O_{7-x}$, in which the strain fluctuations show up as well-developed embryos of the tweed texture and the tweed domains could transform into multitype twins within the CuO layers below the T-O transition temperature.[26] However, our TEM observations of $CaFe_2As_2$ showed that no visible changes of tweed structure were detected along with lowering temperature and going through the T-O transition at 170 K. These facts suggest that the twin lamella and tweed structure in $CaFe_2As_2$ coexisting at low temperature must occur in different atomic layers, i.e., the Fe layers for twin and the Ca layers for tweed, respectively.

As emphasized in Fig. 2, the AFe_2As_2 compounds are composed of two different alternating layers. Our careful structural analysis demonstrates that this pseudoperiodic structural modulation appears only in $CaFe_2As_2$, not in either $BaFe_2As_2$ or $SrFe_2As_2$, considering the smaller size of a Ca^{2+} (0.99 Å) ion in comparison to Sr^{2+} (1.12 Å) and Ba^{2+} (1.34 Å) ions. We suggest that this modulation arises essentially from local structural distortions within the Ca atomic layers, which results in a visible stripe pattern going along the diagonal of Ca squares, i.e., the ⟨110⟩ direction of the tetragonal structure. Taking into account the considerably different physical properties observed in the $CaFe_2As_2$ and $SrFe_2As_2$ compounds, it is likely that the pseudoperiodic structural modulation in $CaFe_2As_2$ could have a certain impact on the structural instability and physical properties. For instance, the anomalies in $CaFe_2As_2$ associated with the SDW instability in both electrical resistivity and magnetic susceptibility show visibly dissimilarities with what is observed in $SrFe_2As_2$ and $BaFe_2As_2$ (Fig. 1).

In summary, the AFe_2As_2 (A=Sr,Ca) compounds show a rich variety of structural phenomena in correlation with the well-known low-temperature T-O phase transition and local structural distortion. The tetragonal $SrFe_2As_2$ samples, consistent with previous x-ray and neutron-diffraction data, undergo the T-O phase transition at about 205 K and show clear

twin domains in the orthorhombic phase. Moreover, TEM observations of $CaFe_2As_2$ reveal the presence of a pseudoperiodic structural modulation at room temperature and this modulation with a wavelength of around 40 nm can be fundamentally interpreted as the local structural distortions within the Ca layers. In the low-temperature orthorhombic phase, the coexistence of twin lamella and tweed structure in general yields complex microstructure features in the *a-b* plane of $CaFe_2As_2$.

This work is supported by the National Science Foundation of China, the Knowledge Innovation Project of the Chinese Academy of Sciences, and the 973 projects of the Ministry of Science and Technology of China.

*Corresponding author. ljq@aphy.iphy.ac.cn

[1] Y. Kamihara, T. Watanabe, M. Hirano, and H. Hosono, J. Am. Chem. Soc. **130**, 3296 (2008).
[2] X. H. Chen, T. Wu, G. Wu, R. H. Liu, H. Chen, and D. F. Fang, Nature (London) **453**, 761 (2008).
[3] G. F. Chen, Z. Li, D. Wu, G. Li, W. Z. Hu, J. Dong, P. Zheng, J. L. Luo, and N. L. Wang, Phys. Rev. Lett. **100**, 247002 (2008).
[4] Z. A. Ren *et al.*, Europhys. Lett. **82**, 57002 (2008).
[5] Z. A. Ren, G. C. Che, X. L. Dong, J. Yang, W. Lu, W. Yi, X. L. Shen, Z. C. Li, L. L. Sun, F. Zhou, and Z. X. Zhao, Europhys. Lett. **83**, 17002 (2008).
[6] C. Wang *et al.*, Europhys. Lett. **83**, 67006 (2008).
[7] M. S. Torikachvili, S. L. Bud'ko, N. Ni, and P. C. Canfield, Phys. Rev. Lett. **101**, 057006 (2008).
[8] M. Rotter, M. Tegel, and D. Johrendt, Phys. Rev. Lett. **101**, 107006 (2008).
[9] A. S. Sefat, R. Jin, M. A. McGuire, B. C. Sales, D. J. Singh, and D. Mandrus, Phys. Rev. Lett. **101**, 117004 (2008).
[10] K. Sasmal, B. Lv, B. Lorenz, A. M. Guloy, F. Chen, Y. Y. Xue, and C. W. Chu, Phys. Rev. Lett. **101**, 107007 (2008).
[11] H. S. Jeevan, Z. Hossain, D. Kasinathan, H. Rosner, C. Geibel, and P. Gegenwart, Phys. Rev. B **78**, 092406 (2008).
[12] G. F. Chen, Z. Li, G. Li, W. Hu, J. Dong, J. Zhou, X. Zhang, P. Zheng, N. Wang, and J. Luo, Chin. Phys. Lett. **25**, 3403 (2008).
[13] J. Dong *et al.*, Europhys. Lett. **83**, 27006 (2008).
[14] C. de la Cruz *et al.*, Nature (London) **453**, 899 (2008).
[15] J. Zhao, W. Ratcliff, J. W. Lynn, G. F. Chen, J. L. Luo, N. L. Wang, J. Hu, and P. Dai, Phys. Rev. B **78**, 140504(R) (2008).
[16] M. Tegel, M. Rotter, V. Weiss, F. M. Schappacher, R. Pöttgen, and D. Johrendt, J. Phys.: Condens. Matter **20**, 452201 (2008).
[17] M. Rotter, M. Tegel, D. Johrendt, I. Schellenberg, W. Hermes, and R. Pöttgen, Phys. Rev. B **78**, 020503(R) (2008).
[18] Q. Huang, Y. Qiu, Wei Bao, J. W. Lynn, M. A. Green, Y. C. Gasparovic, T. Wu, G. Wu, and X. H. Chen, Phys. Rev. Lett. **101**, 257003 (2008).
[19] J.-Q. Yan *et al.*, Phys. Rev. B **78**, 024516 (2008).
[20] N. Ni, S. Nandi, A. Kreyssig, A. I. Goldman, E. D. Mun, S. L. Bud'ko, and P. C. Canfield, Phys. Rev. B **78**, 014523 (2008).
[21] A. I. Goldman, D. N. Argyriou, B. Ouladdiaf, T. Chatterji, A. Kreyssig, S. Nandi, N. Ni, S. L. Bud'ko, P. C. Canfield, and R. J. McQueeney, Phys. Rev. B **78**, 100506(R) (2008).
[22] R. Mittal, Y. Su, S. Rols, T. Chatterji, S. L. Chaplot, H. Schober, M. Rotter, D. Johrendt, and Th. Brueckel, Phys. Rev. B **78**, 104514 (2008).
[23] P. C. Canfield and I. R. Fisher, J. Cryst. Growth **225**, 155 (2001).
[24] S. Muto, S. Takeda, R. Oshima, and F. E. Fujita, J. Phys.: Condens. Matter **1**, 9971 (1989).
[25] Y. Zhu, M. Suenaga, and A. R. Moodenbaugh, Ultramicroscopy **37**, 341 (1991).
[26] S. Semenovskaya and A. G. Khachaturyan, Phys. Rev. B **46**, 6511 (1992).